AN IMPROVED FORMULATION OF THE BRAY-MOSS-LIBBY (BML) MODEL FOR SI ENGINE COMBUSTION MODELING

C.P. Ranasinghe* and W. Malalasekera**
chathura@mech.mrt.ac.lk
* Department of Mechanical Engineering, University of Moratuwa,
Katubedda, Moratuwa, Sri Lanka
** Wolfson School of Mechanical and Manufacturing Engineering,
Loughborough University, Loughborough, Leics LE11 3TU, UK.

Abstract
In this paper an improved version of the BML model has been developed so that it could be applied to wall-bounded combustion modelling, eliminating the wall flame acceleration problem. Based on the Kolmogorov-Petrovski-Piskunov (KPP) analysis and fractal theory, a new dynamic formulation has been proposed to evaluate the mean flame wrinkling scale making necessary allowance for spatial inhomogeneity of turbulence. A novel empirical correlation has been derived based on experimentally estimated flame image data to quantify the quenching rates near solid boundaries. The proposed modifications were then applied to simulate premixed combustion in two spark ignition engines with different operating conditions. Results show that the present improvements have been successful in eliminating the wall flame acceleration problem found with the original BML model, while accurately predicting the in-cylinder pressure rise, mass burn rates and heat release rates.

Introduction
Computational Fluid Dynamics (CFD) modelling of flow and combustion characteristics in Internal Combustion (IC) engines has been a topic of great research interest. Several models with varying complexity have been developed for modelling combustion in premixed charged Spark Ignition (SI) engines [1-5]. The well-known Bray-Moss-Libby [6] (BML) flame surface density (FSD) model has also been used for premixed combustion modelling for many years. Application of the original BML model [6] for the simulation of open-stagnation flames has shown to be capable of producing good results. However, its application to wall bounded combustion problems are rare due to the wall flame acceleration problem or in simple terms, predicting excessively high unphysical reaction rates near solid boundaries. In fact, this is a common problem of many combustion models and often near wall corrective measures are incorporated.

In this work, the near wall flame acceleration problem in BML type models is addressed. New correlations are developed, which can provide necessary allowance for the inhomogeneity of turbulence and thermal quenching near solid walls. The novel formulation is used to analyse the combustion process in SI engines, as it is one of the most practically important cases of wall bounded premixed combustion. Moreover, the evaluation of several BML model constants is made to be dynamic, so that only a single adjustable constant is left for fine-tuning. It should also be noted that, even though the present approach is demonstrated with the BML model, it can be easily adapted with other RANS based turbulence combustion models as well.

The BML Model

According to the BML model, FSD is given by:

$$\Sigma = \frac{g\bar{c}(1-\bar{c})}{l_y} = \frac{g}{|\sigma_y|}\frac{\bar{c}(1-\bar{c})}{C_b l_i (S_l/u')^n} \tag{1}$$

where, Σ is flame surface density, l_y the integral scale of flame wrinkling, u' is the turbulence intensity and $\bar{c}$ the mean progress variable of the reaction. In the expanded expression, g, C_b and σ_y are model constants, l_i is the integral scale of turbulence and S_l is the laminar flame speed. σ_y is taken to be 0.7 as suggested in [7-9]. $g = 2$ if the mean spatial distribution of flamelet crossing points on the iso-$\bar{c}$ surface is exponential. If it has a symmetric beta probability distribution then $g = 1$. In practice, flamelet crossing distribution is found to vary in-between symmetric and exponential range. However, Chew *et al* [8] and Patel & Ibrahim [11] showed that scatter of crossing lengths are more biased towards an exponential distribution with an average g value of 1.7-2.0. Further, it has been suggested [10,11] that the variation of g with the progress of reaction can be better expressed by using $g = 1 + 2\bar{c}$. This has been adopted in this study. The integral scale of turbulence is given by $l_i = c_l\left(u'^3/\varepsilon\right)$. The proportionality constant $c_l \approx 0.76$, ε is the turbulence kinetic energy dissipation rate.

The scatter of the values of model parameters C_b and n, in Eq. (1) is so wide [7-13] and no reasonable mean value could be specified. For n, values such as 1.0, 1.2, 0.36 and 0.41 can be found in the literature [7, 9, 12, 13]. Also for C_b, a value of 0.23 has been suggested in [7] and 12.3 in [9]. Difficulty of finding reasonable values for C_b and n, has been a major complexity with the standard BML model.

Application of the standard BML model in wall-bounded systems is very rare due to the problem of near wall flame acceleration. Physically, this is unrealistic, as flames tend to extinguish at walls due to thermal quenching. BML model also assumes isotropic homogeneous turbulence. Thus, its application in the core region of the flame, where sufficiently homogeneous turbulence exists results in satisfactory results. Close to solid walls, the turbulent intensity u' rapidly decreases towards zero, which eventually leads to very small values of the integral scale given by $l_i \sim u'^3/\varepsilon$. As a result, the flame surface density in Eq.(1) becomes very large, so does the reaction rate. To overcome this unphysical nature of the original BML model, alternative expressions have been proposed [14, 15]. In these models, the flame wrinkling is assumed to be an empirical function of the laminar flame thickness and u'. The fundamental disadvantage of these models is that they neglect the well-known direct dependency of flame wrinkling on the integral scale.

A Dynamic Model for the Evaluation of Flame Wrinkling Scale

In this section, the turbulent flame speeds of the BML model and the Fractal Flame combustion model (FFM) given by the Kolmogorov–Pertovsky–Piskunow (KPP) analysis are evaluated and a new expression for the BML model constant n is derived. Only the major steps of the derivation are shown here and the interested readers may refer [16-18] for more details. According to the KPP analysis, an expression for $S_{t,BML}$, the turbulent burning velocity predicted by the BML model can be derived as:

$$S_{t,BML} = \left[4C_{eff}u'I_0S_l\frac{g}{|\sigma_y|}\frac{1+\tau}{C_b(S_l/u')^n}\right]^{0.5} \tag{2}$$

τ is the heat release factor and the C_{eff} is a constant. Using fractal theories, an expression for the turbulent flame speed may be derived as:

$$S_{t,FFM} = C_t I_0' S_l (\epsilon_0/\epsilon_i)^{D-2} \tag{3}$$

Here D is the fractal dimension, I_0' the stretch factor and ϵ_0 and ϵ_i are outer and inner cut-off scales. In the early stage of fractal modelling the parameter C_t was considered to be a constant. However, later it was recognized that this would result in modelling deficiencies [19, 20]. Therefore, C_t can be more accurately interpreted by assuming proportionality to $(u'/S_l)^{0.5}$, giving $C_t = C_t'(u'/S_l)^{0.5}$ where C_t' is a model constant.

If the minimum (ϵ_i) and maximum (ϵ_0) scales of flame wrinkling is represented using the Gibson scale $(l_G = S_l^3/\varepsilon)$ and the integral scale respectively, the wrinkling scale becomes,

$$\left(\frac{\epsilon_0}{\epsilon_i}\right)^{D-2} = C_G^{D-2}\left(\frac{u'}{S_l}\right)^{3(D-2)} \tag{4}$$

D is the fractal dimension and C_G^{D-2} is a constant. Equating turbulent flame speeds given by the two models the following relation is obtained.

$$C_t' I_0' C_G^{D-2}\left(\frac{u'}{S_l}\right)^{0.5} \frac{{u'}^{3(D-2)}}{{S_l}^{3D-7}} = \left[4C_{eff} I_0 \frac{g}{|\sigma_y|}\frac{1+\tau}{C_b}\left(\frac{{u'}^{n+1}}{{S_l}^{n-1}}\right)\right]^{0.5} \tag{5}$$

By comparing dimensions of both sides of the equation, it can be shown that $n = 6D - 12$. It is noted that in Bray's original model [12], C_t was assumed to be a constant. The inner and outer flame wrinkling scales were assumed to be integral and Gibson scales respectively. This resulted in $n = 6D - 13$. Further, D was assumed to be a constant with a value $D = 7/3$ giving a value of $n = 1$.

The advantage of this new formulation is that, for small values of u': such as near walls, n tends to zero, making the term $(S_l/u')^n$ tending to unity. For SI engine applications D is a variable. Thus, the use of a dynamic fractal dimension that can adjust itself according to in-cylinder conditions is essential. For this the relation suggested in [20], for D has such dynamic properties and used in the present modified form of the BML model.

$$D = 2.05\frac{200}{200 + Re_t} + 2.35\frac{Re_t}{200 + Re_t} \tag{6}$$

The main reason for the near wall singularity of the BML model is that, it uses the classical definition of the integral scale to calculate l_y given in Eq.(1). For practical applications, corrections must be made to account for inhomogeneity. Sreenivasan's [21] compared several experimental data sets of grid generated turbulence length scales and a functional dependence between the Taylor Reynolds number(Re_λ) and the turbulent integral scale constant c_l was found. Based on the observations in [21], Lindsted & Vaos [22] obtained the following curve-fit for c_l.

$$c_l = 1 + a/Re_\lambda + b/{Re_\lambda}^2 \tag{7}$$

where $a = 5.715$ and $b = 72.051$ respectively. This expression has been used in the present study for the modelling of the integral scale of turbulence. One of the main advantages of this

expression is that it eliminates the singularity of the BML model at near zero turbulent intensities.

A Model for Flame Quenching at Solid Walls

A flame front is quenched when it approaches a cold wall due to excessive heat loss. Rate of quenching is determined by the relative intensity of heat release from combustion and the rate of absorption of heat by the cold boundary. There exist two distinct quenching regions [23-25] near walls. Closest to the wall, a total quenching region exists in which no reaction is ever taken place. In the influence zone: region above the total quenching region, the flame front senses the presence of the wall and is subjected to partial quenching. According to DNS results in [23] the thickness of the quenching zone corresponds to a Peclet number of 3.5 and that of influence zone is 10. Here the Peclet number (Pe) is defined as the ratio of the flame power to the wall heat flux. A simplified expression for Pe may be obtained as $Pe = d/\delta$ where d is distance from the wall and δ is the laminar flame thickness. Experimental investigations in [24] and [25] provide an insight into the understanding of flame wall interaction. Laser tomographic images taken during head-on quenching in an optical engine has revealed the influence zone thickness could be as high as 40 times the quenching zone thickness, which is quite large compared to the DNS findings.

For the influenced zone, the quenching rate parameter QR has been defined as the ratio between the length of the active flame and the total flame length.

$$QR = l_f/(l_f + l_q) \tag{8}$$

where, l_f and l_q are respectively the active length and the quenched length of the flame front for a given flamelet segment. Partial flame quenching results in reduced burning rates and incomplete combustion. This suggests the necessity of introducing the wall-flame quenching effects into the burning rate integral in modeling studies. It has been experimentally verified that burning rate in the vicinity of a solid wall can be expressed in terms of the quenching rate as [25]:

$$\bar{\dot{\omega}}_w = \bar{\dot{\omega}} \times QR \tag{9}$$

where $\bar{\dot{\omega}}_w$ is the near wall unburned gas consumption rate and $\bar{\dot{\omega}}$ is the unburned gas consumption rate in the absence of quenching. The observed trend in the variation of quenching rate with d for equivalence ratios (ϕ) of methane air mixtures was found to be reasonably linear near the wall and then exponentially decay towards unity at the outer boundary of the influenced zone. In order to implement these findings in a computer code a functional formulation is needed. It was found during the present work that these results can be correlated quite well with the following expressions.

Let, non-dimensional normalized distance $\mathcal{D}_Q$ be taken as;

$$\mathcal{D}_Q = \frac{d - d_{cr}}{d_{max} - d_{cr}} \qquad 0 \le \mathcal{D}_Q \le 1 \tag{10}$$

where, d_{cr} is the thickness of the total quenching zone and d_{max} is the distance to the outer boundary of the influenced zone. Then the experimental QR values can be best fitted with following relations.

$$QR = 1.0 - 2.0/\left[1 + \exp(\mathcal{D}_Q)^{\alpha}\right] \tag{11}$$

$$\alpha = \beta/\left(1.0 - 0.6\mathcal{D}_Q\right) \text{ and } \beta = 3.7 - 2|\phi - 1.0| \tag{12}$$

Here β varies with operating conditions. Expression for β is arrived based on the assumption that the minimum rate of quenching occurs at $\phi = 1$. This assumption is valid as the variation of quenching Peclet number (Pe_Q) of many of the fuels is symmetric about $\phi = 1$ or has only a small offset [26]. For much accurate calculations, a fuel specific determination of β is needed. However, due to the unavailability of experimental data, the trend shown [25] is assumed for all types of fuels.

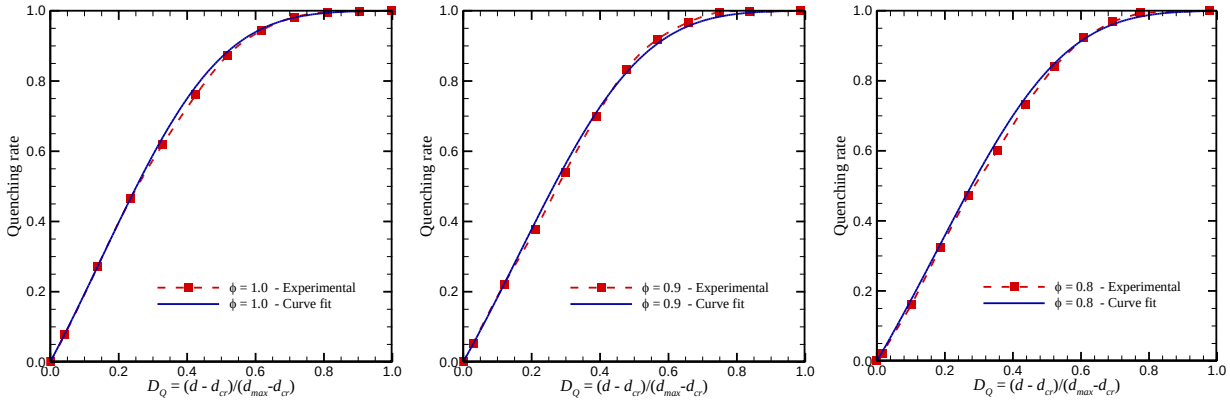

(a) $\phi = 1.0$ and $\beta = 3.7$ (b) $\phi = 0.9$ and $\beta = 3.5$ (c) $\phi = 0.8$ and $\beta = 3.3$

Figure 1. Experimental and curve fitted quenching rate

Figure 1(a-c) show the comparison of curve fitted graphs using the expression suggested in Eqns.(11,12). It can be seen that the agreement is remarkably good for the entire zone in each case.

The usual practice in wall quenching studies is to represent the parameters in terms of Pe. The quenching zone, is so small such that the variation of temperature, pressure and the other fluid properties is negligible [26]. Thus, the laminar burning velocity and the kinematic viscosity of the fluid can also be considered constant and hence the laminar flame thickness (δ).

Normalizing Eq.(10) with respect to δ leads:

$$\mathcal{D}_Q = (d/\delta - d_{cr}/\delta)/(d_{max}/\delta - d_{cr}/\delta) \tag{13}$$

Using $Pe = d/\delta$, $\mathcal{D}$ is obtained in terms of Peclet number as:

$$\mathcal{D}_Q = (Pe - Pe_{cr})/(Pe_{max} - Pe_{cr}) \tag{14}$$

The critical Peclet number (Pe_{cr}) is usually termed the quenching Peclet number (Pe_Q) in the literature. The following empirical expression used in this study is from [27].

$$Pe_Q = (1.9/\phi)(p/3)^{0.26\min(1\,,1/\phi^2)} \tag{15}$$

This expression does not account for the effect of temperature variations on quenching, which should essentially be embedded.

Only a limited number of studies have been carried out to investigate the limits of maximum quenching distance. Among those, [24] and [25] are the only available experimental evidence for quenching distances in engine combustion. As the aim of the present study is to model the premixed combustion in SI engines, Pe_{max} is taken to be 40 times Pe_Q as found in [24].

Modelling the Reaction Rate

In this section, the application of the modified BML formulation with proposed improvements to model the premixed combustion in SI engines is discussed. The final model form used in evaluating the unburned gas consumption rate is given by;

$$\bar{\dot{\omega}} = \frac{C_{BML}\rho_u I_0 S_l}{|\sigma_y|} \frac{(1+2\bar{c})\bar{c}(1-\bar{c})QR}{\left(1+\frac{a}{Re_\lambda}+\frac{b}{{Re_\lambda}^2}\right)\frac{u'^3}{\varepsilon}\left(\frac{S_l}{u'}\right)^{6D-12}} \tag{16}$$

C_{BML} is an integrated model constant. Flame stretching factor I_0 was modelled as in [28]. The correlation in [29] was used to calculate the unstrained laminar burning velocity. The above model was implemented in the KIVA4 CFD code [30], which is capable of solving compressible Navier –Stokes equations in unstructured meshes with moving boundaries. Governing equations were solved in an Arbitrary Lagrangian Eularian framework with the standard $k-\varepsilon$ turbulence model. Fuel oxidisation is considered to be a simple one-step reaction. Spark ignition and flame kernel development was simulated using the Discrete Particle Ignition Kernel (DPIK) model [31].

As an initial validation of the new formulation, Propane combustion in the General Motors (GM) research engine [32] was modelled. This engine has a pancake combustion chamber with a centrally located spark plug. Then the validation was extended to the modelling of full cycle combustion process in a Ricardo E6 single cylinder engine. Unstructured hexahedral meshes were used in both cases. In both cases, the squish region alone contained around 100,000 computational cells, which corresponds to a cell dimension in the order of 1mm. Further details on this modelling work can be found in [18].

Subsequently, the model was applied to the Ricardo E6 engine. Simulations of the Ricardo engine were started at 20 BTDC on the exhaust stroke. Initial properties and mass fractions were calculated using a thermodynamic analysis. Based on exhaust gas temperature measurements, in-cylinder and exhaust gas mixture temperatures of the Ricardo E6 engine were taken to be 750K at the start of simulation. In cylinder, fluid and turbulent properties were homogeneously initialized except the dissipation rate of turbulent kinetic energy, which was taken to be inversely proportional to the distance from the cylinder wall. Intake manifold pressure was slightly adjusted such that the trapped in-cylinder air and fuel masses were equal to the measured quantities.

Results and Discussion

Flame propagation near solid walls in the GM engine was examined with the aim of assessing the suitability of the present improved BML model in predicting wall-bounded combustion. As a reference case, the standard BML model (MF1) with classical definition for the integral scale with the constant $n = 1$ was used and the resultant flame evolution is shown in the first row of Figure 2. The second row depicts the prediction of the new BML model without the wall-quenching model (MF2). Illustrated in the third row is the complete model results, which comprises of the dynamic calculation of model constants and the quenching model (MF3).

Figure 2 shows the variation of the burned fuel mass fraction (x_b) across an axial cross sectional plane in the engine cylinder with the crank angle. Reacting zone may be identified as the region between $x_b = 0$ and $x_b = 1$. Excessive flame acceleration with the standard BML model (MF1) is apparent even from the very early stages of the combustion process. This is noticeable in the figure corresponding to -5ATDC where the x_b reaches 1.0 much faster on the piston surface compared to the core region. As a result, the shape of the flame front propagation is seen to be concave in the inner region and nearly flat in the leading front, where in reality both these regions are observed to be convex.

As shown in row 2 the introduction of the dynamic calculation of model constants (MF2) makes a considerable improvement over MF1 and results in a more physical convex and outward flame front. However, in the vicinity of the walls a comparatively high rate of reaction can still be seen. Although the dynamic evaluation of model constants makes a big improvement over MF1, at walls where u' becomes so small it damps the effects of dynamically calculated c_l and n values.

As shown in the third row, employment of the new quenching correlation (MF3) successfully hinders the flame wall acceleration and makes the flame front agreeably convex. In addition, the flame brush thickness is seen to be much thinner compared to other model, and now more acceptable in this type of low turbulence engines. These observations are in good agreement with the optical imaging results reported in [33].

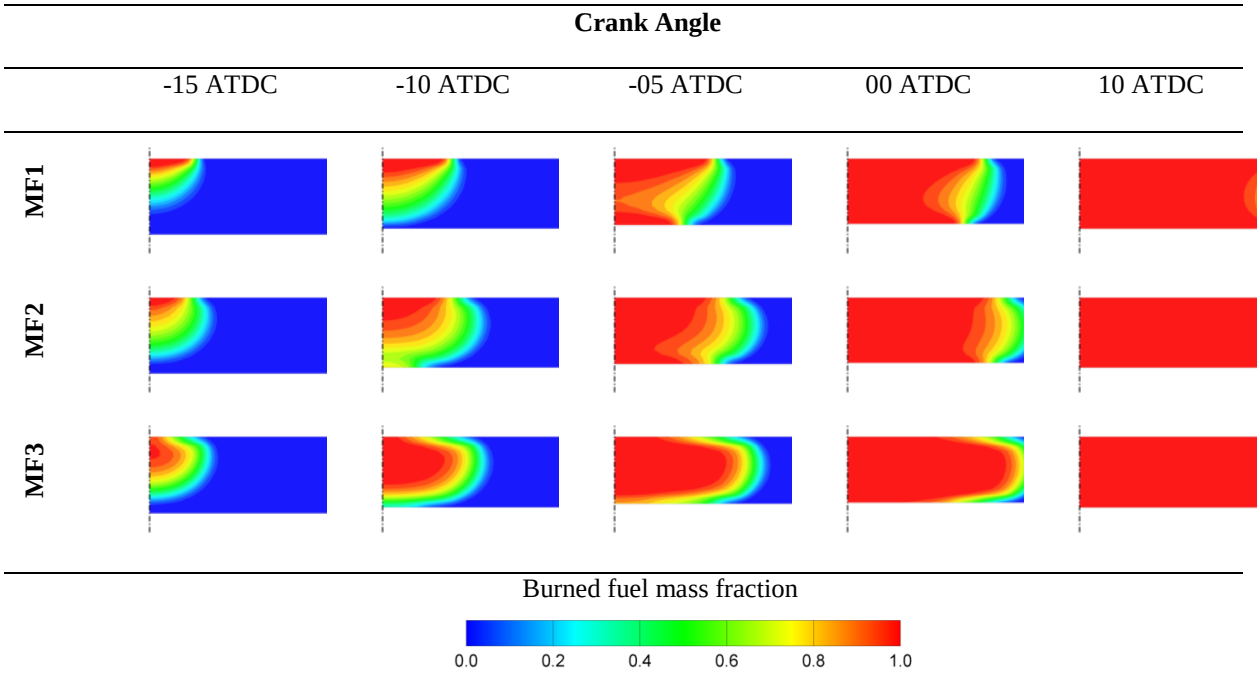

Figure 2. Flame propagation in the GM engine

Shown in Figs. 3 and 4 are the predicted and measured pressure and mass burn data of the GM engine for the two test cases considered. In this simulation C_{BML}, was set to be 1.23. It can be seen that computed results are very much encouraging and they are in close agreement for the cases shown and the agreement is good for other test cases as well [18]. However in general, a slight difference in the peak pressure location is seen. Calculated x_b values are also in good agreement with the experimentally derived values, up to a cumulative value of about 80%. Beyond this point, an over prediction of x_b is seen from the calculated results.

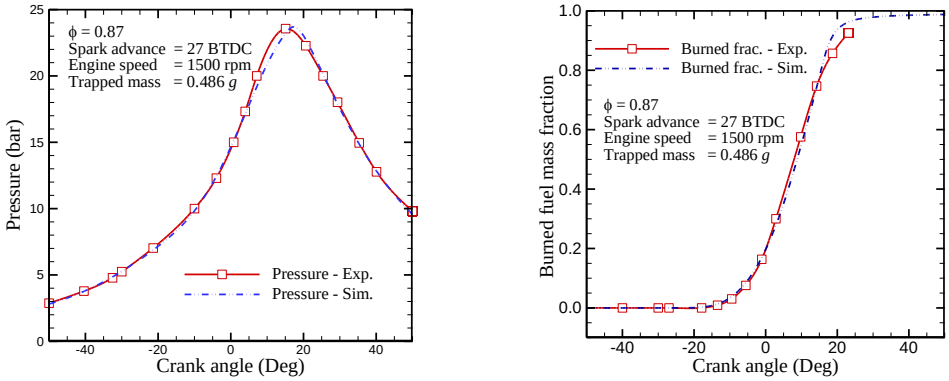

Figure 3. In-cylinder pressure rise and fuel burned fuel mass fraction: case 1

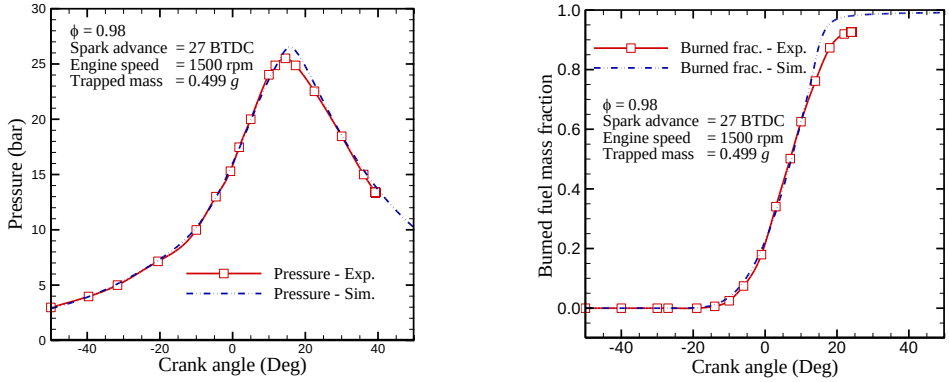

Figure 4. In-cylinder pressure rise and fuel burned fuel mass fraction: case 2

Next, the results from the full cycle engine simulation of E6 engine are discussed. Figure 5(a) shows the computational mesh of the engine used and the Figure 5(b) show the velocity distribution inside the engine cylinder in a plane across the intake valve. Illustrated in Figure 5(c) is the calculated in cylinder turbulent kinetic energy in a plane through the spark plug location. In the vicinity of the spark plug turbulence levels appear to be less intense compared to the core region of the cylinder.

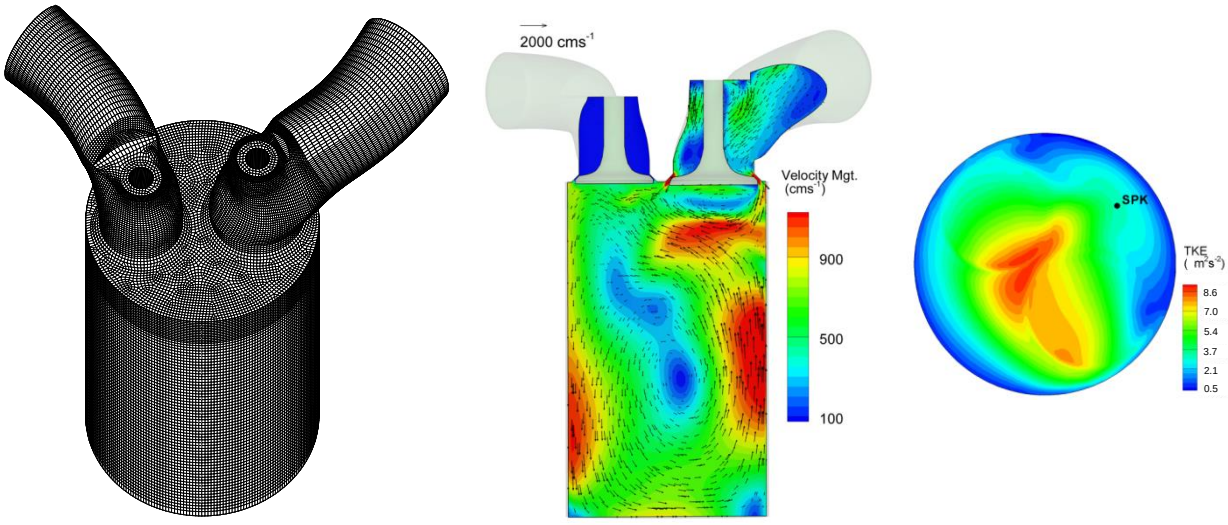

(a) (b) (c)

Figure 5. (a) Unstructured hexahedral mesh of the E6 engine
(b) Velcoty profile in a cut plane cross the intake valve at piston BDC
(c) Turbulent kinetic energy profile in the spark location plane at 344 CAD

The near wall intensity of the turbulent kinetic energy is approximately about 15 times smaller than the core region value. Hence, the conventional approach of the BML model would have resulted in flame wall acceleration if applied to this test case.

In the application of the new BML model, C_{BML} was set to 2.15 for all the test cases. Pressure trace predictions and heat release rates are compared with the experimental values and shown in Figures 6 and 7. In general, the predicted and simulated traces of in-cylinder pressure are in good agreement. The model has precisely captured the trends in in-cylinder pressure variation for different engine operating conditions. Estimation of the peak pressure is reasonably accurate. Both the predicted and experimental magnitude of the peak heat release rates (HRR) and the cumulative heat release rates (CHR) are in close agreement, only a slight shift in the maximum HRR location is observed.

As in the GM engine, it is noted that the model over predict the pressure trace during the last stage of combustion. This is probably be due to the absence of a blow- by gas model in the present study. In the first case where there is a higher peak pressure and a lower engine speed, the over prediction is much apparent compared to the second case where engine speed is higher and the peak pressure is lower. In the second case, as less time and a lower peak pressure is available less blow-by mass is expected, therefore the predictions closely follows the experimental trace. In general, the overall agreement in the pressure predictions during the early and middle stage of the engine cycle is very good for both cases indicating the success in combustion predictions.

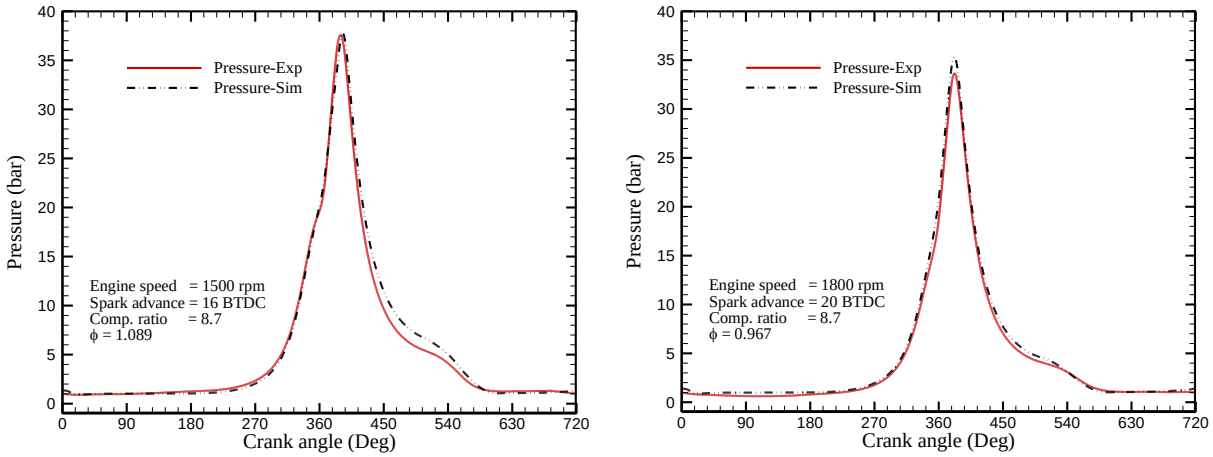

Figure 6. In-cylinder pressure rise : Ricardo E6 Case 1 & Case 2

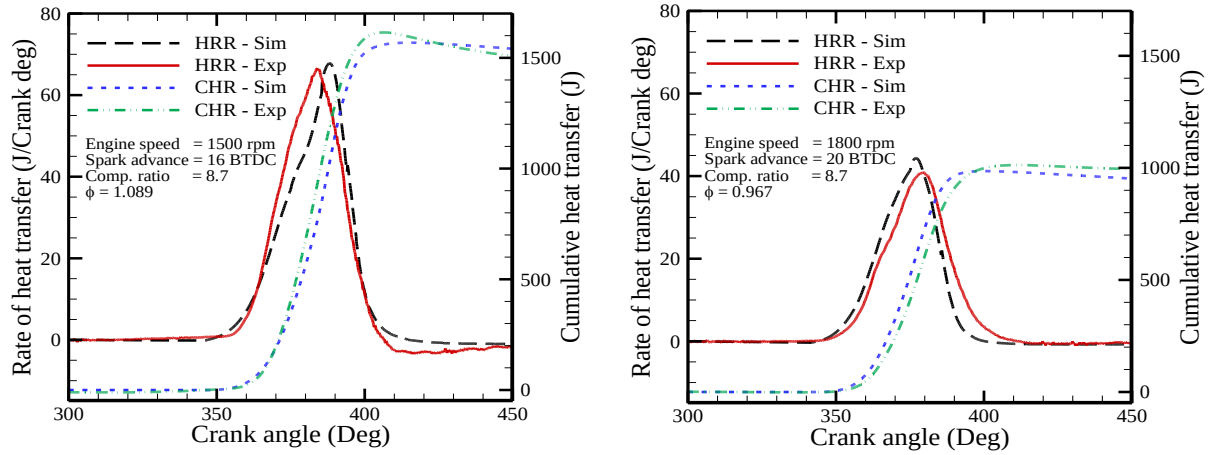

Figure 7. Heat release rate due to combustion: Ricardo E6 Case 1 & Case 2

Conclusions

Standard BML model produces poor results in wall bounded combustion, as it suffers from the near wall flame acceleration problem. Also, it involves several adjustable model constants which need case by case fine tuning. In this study a new comprehensive model based on the BML model was developed which can compute required model constants dynamically leaving a single constant to be specified. Further improvements were made to eliminate near wall flame acceleration problem of the BML model. A new empirical correlation was derived to account for the effect of quenching on the combustion rate near solid boundaries.

The new model formulation was then tested for predicting premixed combustion in SI engines. Simulations show that the new model has successfully captured the experimentally observed flame front evolution. It has the capability of accurately calculating the near wall reaction rates eliminating the wall flame acceleration problem. The proposed quenching rate model has also shown to predict better results. Engine simulations with the present improved version of the BML model shows that it can satisfactorily predicted the experimentally observed pressure values, mass burn rates and heat release rates.

Nomenclature

$\bar{c}$	Mean progress variable
d	Distance from the solid boundary
D	Fractal dimension in three dimension
$\mathcal{D}$	Normalized quenching distance
I_0	Flame front wrinkling factor
l_f	Active flamelet length
l_i	Integral length scale of turbulence
l_q	Quenched flamelet length
l_y	Flamelet wrinkling scale
Pe	Peclet Number
QR	Quenching rate
Re_λ	Taylor Reynolds Number
S_l	Laminar burning velocity
S_t	Turbulent burning velocity
u'	Turbulent intensity
δ	Laminar flame thickness
ε	Dissipation rate of turbulent kinetic energy
Σ	Flame surface density
τ	Heat release factor
ϕ	Equivalence ratio
$\overline{\dot{\omega}}$	Unburned mass consumption rate
ϵ_0	Outer cut off scale
ϵ_i	Inner cut off scale

Subscripts

u	Unburned
cr	Critical
max	Maximum
in	Intake
$wall$	Near/On wall
Q	At quenching

References

[1] Magnussen, B.F., Hjertager, B.H., "On mathematical modeling of turbulent combustion with special emphasis on soot formation and combustion", *Proc. Combust. Inst*. 16: 719-729(1977).

[2] Spalding, B., "Development of the eddy-break-up model of turbulent combustion", *Proc. Combust. Inst.* 16:1657-1663(1977).

[3] Marble, F.E., Broadwell, J.E., "The coherent flame model for turbulent chemical reactions", Technical Report: TRW-9-PU, Project Squid, (1977)

[4] Boudier, P., Henriot. S., Poinsot. T., Baritaud. T., "A model for turbulent flame ignition and propagation in spark ignition engines". *Proc. Combust. Inst*. 24:503-510(1992).

[5] Ewald, J., Peters, N., "A level set based flamelet model for the prediction of combustion in spark ignition engines." *15th International Multidimensional Engine Modeling User's Group Meeting*, Detroit, MI. (2005).

[6] Bray, K.N.C., Champion, M., Libby, P.A., "The interaction between turbulent and chemistry in premixed turbulent flames", *In Turbulent Reacting Flows (R. Borghi, S.N.B., Murthy Eds)*, Springer Verlag, Berlin, 541-563 (1989).

[7] Chang, N.W, Shy, S.S., Yang, S.I., Yang, T.S., "Spatially resolved flamelet statistics for reaction rate modeling using premixed methane-air flames in a near-homogeneous turbulence." *Combust. Flame* 127:1880 – 1894(2001).

[8] Lahjaily, H., Champion, M., Karmed, D., Bruel, P., "Introduction of dilution in the BML model: application to a stagnating turbulent flame", *Combust. Sci. & Tech.* 135:153-173:(1998).

[9] Shy, S.S., Jang, R.H., I,W.K., Gee, K.L., "Three-dimensional spatial flamelet statistics for premixed turbulent combustion modeling."*Proc. Combust. Inst.* 26: 283-289(1996).

[10] Chew, T. C., Bray, K. N. C., Britter., R. E., "Spatially resolved flamelet statistics for reaction rate modeling." *Combust. Flame*,80: 65-82(1990).

[11] Patel, S.N.D.H., Ibrahim, S.S., "Calculations of burning velocity of turbulent premixed flames using a flame surface density model", *JSME International J*., Series – B, 45 725-735 (2002).

[12] Bray, K.N.C., "Studies of the Turbulent burning velocity", *Proceedings of the Mathematical and Physical Science*, 431:315-335(1990).

[13] Aluri, N.K., Pantangi, P.K.G., Muppala, S.R.P., Dinkelacker, "A numerical study promoting algebraic models for the Lewis number effect in atmospheric turbulent premixed Bunsen flames", *Flow Turb. and Combust.* 75:149-172(2005).

[14] Watkins, A.P., Li, S.P., Cant, R.S., "Premixed combustion modelling for spark ignition engine applications", *SAE Paper*: 961190 (1996).

[15] Abu-Orf, G.M., Cant, R.S, "A turbulent reaction rate model for premixed turbulent combustion in spark-ignition engines", *Combust. Flame*, 252:122-133(2000).

[16] Poinsot, T., Veynante, D., "Theoretical and Numerical Combustion", Edwards, ISBN: 1-930217-05-6,(2001).

[17] Ranasinghe, C.P., Malalsekera, W., "Simulation of premixed combustion and near wall flame quenching in spark ignition engines with an improved formulation of the Bray-Moss-Libby Model", *9th International Conference HEFAT*, Malta ,1-5, ISBN: 9781868549863, (2012).

[18] Ranasinghe, C.P., "Development of combustion models for RANS and LES applications in SI Engines", PhD Thesis, Loughborough University, UK, (2013).

[19] Gülder,Ö.L., Smallwood,G.J., "Do turbulent premixed flame fronts in spark-ignition engines behave like passive surfaces?", *SAE Paper* :2000-01-1942, (2000).

[20] Zhao, X., Matthews, R.D., Ellzey, J.L., "Numerical simulations of combustion in SI engines: comparison of fractal flame model to the coherent flame model", *Int. Symp. COMODIA*, (1994).
[21] Sreenivasan, K.R., "On the scaling of the turbulent energy dissipation rate", *Phy. of Fluids*, 27:1048-1051(1984).
[22] Lindstedt, R. P., E. M. Váos. "Modeling of premixed turbulent flames with second moment methods." *Combust. Flame* 116.4: 461-485(1999).
[23] Poinsot, T. J., D. C. Haworth, and G. Bruneaux. "Direct simulation and modeling of flame-wall interaction for premixed turbulent combustion", *Combust. Flame*, 95.1-2:118-132(1993).
[24] Foucher, F., Brunel, S., Rousselle, M., "Evaluation of burning rates in the vicinity of the piston in a spark-ignition engines, *Proc. Combust. Inst.*, 29:751-757(2002).
[25] Foucher, F., Mounaïm-Rousselle, C. "Fractal approach to the evaluation of burning rates in the vicinity of the piston in a spark-ignition engine". *Combust. flame*, 143: 323-332.(2005).
[26] Karrer, M., Bellenoue, M., Labuda, S., Sotton, J., Makarov, M., "Electrical probe diagnostics for the laminar flame quenching distance", *Exp. Thermal and Fluid Science*, 34:131-141(2010).
[27] Lavoie, G.A., "Correlation of combustion data for SI engine calculations – laminar flame speed, quenching distance and global reaction rate", *SAE Paper:* 780229, (1978).
[28] Law, C. K., D. L. Zhu, and G. Yu. "Propagation and extinction of stretched premixed flames." *Proc. Combust. Inst* , 21(1988.)
[29] Gülder, Ö.L., "Correlation of laminar combustion data for alternative SI engine fuels". *SAE Paper:* 841000, (1984).
[30] Torres, D.J., Trujillo, M.F, "KIVA-4: An Unstructured ALE Code for Compressible Gas Flow with Sprays", *J. of Comp. Physics*, 216:943-975(2006).
[31] Fan, L., Reitz, R.D., "Development of an ignition and combustion model for spark-ignition engines", *SAE Paper:* 2000-01-2809, (2000).
[32] Kuo, T.W., Reitz, R.D., "Computation of premixed-charge combustion in pancake and pent-roof engines", *SAE Paper* : 890670,(1989).
[33] Weller, H.G. Uslu, S. Gosman, A.D., Maly, R.R., Herweg, R., Heel, B., "Prediction of combustion in homogeneous-charge spark-ignition engines", *Int. Symp. COMODIA*, (1994).